

**SLOVAK UNIVERSITY OF TECHNOLOGY IN BRATISLAVA  
FACULTY OF ELECTRICAL ENGINEERING  
AND INFORMATION TECHNOLOGY**

Student's ID: 56727

**COMBINING SURFACE AND VERTICAL PROFILE-STUDIES  
OF ORGANIC MATERIALS IN SOLAR CELLS**

**DISSERTATION THESIS SUMMARY**

Study programme:      Microelectronics  
Study field ID:        5.2.13. Electronics  
Study field:            Electronics  
Work place:            STU, ILC and JKU  
Thesis supervisor:    prof. Ing. František Uherek, PhD.  
Consultant             Ing. Andrej Vincze, PhD.

**Bratislava, 2015**

**MSc. Mamadou Seck**

Dizertačná práca bola vypracovaná v dennej forme doktorandského štúdia na Ústave elektroniky a fotoniky Fakulty elektrotechniky a informatiky Slovenskej technickej univerzity v Bratislave.

Predkladateľ: **MSc. Mamadou Seck**  
Slovenská technická univerzita, Fakulta elektrotechniky a informatiky  
Ústav elektroniky a fotoniky  
Ilkovičova 3, 812 19 Bratislava

Školiteľ: **Prof. Ing. Frantisek Uherek, PhD.**  
Slovenská technická univerzita, Fakulta elektrotechniky a informatiky  
Ústav elektroniky a fotoniky  
Ilkovičova 3, 812 19 Bratislava

**Ing. Andrej Vincze, PhD.**  
Medzinárodné laserové centrum  
Ilkovičova 3, 841 04 Bratislava

Oponenti: **RNDr. Eva Majková, DrSc.**  
Slovenská akadémia vied  
Štefánikova 49  
814 38 Bratislava

**Prof. Ing. Siegfried Bauer, PhD.**  
Department of Soft Matter Physics (SoMap)  
Johannes-Kepler-University Linz  
Altenbergerstrs. 69 A-4040 Linz

Autoreferát bol rozoslaný dňa:

Obhajoba dizertačnej práce sa koná:                    o                    hod.

na Fakulte elektrotechniky a informatiky STU v Bratislave, Ilkovičova 3, blok E, 6. poschodie

**prof. Dr. Ing. Miloš Oravec**  
dekan FEI STU

## Abstrakt

V uplynulých rokoch sa atraktivnosť technológií organických solárnych článkov zvýšila z dôvodu ich zásadných výhod akými sú relatívne nízke náklady na spracovanie a prípravu, použitie nízkoenergetickej polymérnej chémie, flexibilita prípravy prakticky na čokoľvek, nízka hmotnosť a transparentnosť štruktúr. Napriek tomu, pokračujúci intenzívny výskum stále nie je uzavretý, aby sa našli a vyjasnili procesy degradácie aktuálne používaných materiálov za štandardizovaných pracovných podmienok. Toto úsilie je vynakladané z dôvodu dosiahnutia vyššej stability organických solárnych prvkov pre aplikácie v rôznych oblastiach. Zabudovanie nových p-typ polymérov do štruktúr s nízkou energetickou medzerou dovoľuje zvýšenie absorpcie v červenej oblasti slnečného spektra, a teda aj účinnosť zariadenia, ktorá aktuálne dosahuje hodnoty nad 13%. Fotoaktívna vrstva sa skladá z p-typ polyméru, ktoré sú zmiešané spolu s n-typ polymérmi, ktorých typickým predstaviteľom sú fularénové deriváty.

Materiály použité v fotoaktívnej vrstve nie sú stabilné za štandardných podmienok a majú tendenciu sa rozkladať, ako bolo ukázané v literatúre rôznymi výskumnými skupinami. Typické pracovné podmienky organických solárnych článkov sú také, kde sú vystavené vysokým teplotám, zmenám relatívnej vlhkosti okolitej atmosféry, intenzívnym zmenám dopadajúceho svetelného žiarenia so silnou UV zložkou atď. Tieto podmienky vedú k chemickej a fyzikálnej degradácii, napr. vytváraniu tripletových formácií pri prenose náboja, produkcie kyslíka, oxidácií polyméru, oxidácie elektród, svetlom-žiarením asistovanej dopácií s O<sub>2</sub>, morfológických zmien, reakcií medzi vrstvami, delaminácií, difúzií O<sub>2</sub> a H<sub>2</sub>O v štruktúre. Tieto degradačné procesy sa väčšinou odohrávajú vo fotoaktívnej vrstve. Spoločný degradačný proces kyslíka so svetelným žiarením je známy ako fotooxidácia a predstavuje hlavný dôvod zlyhania prvku. Fotooxidácia vplýva na parametre morfológie vrstiev, ako aj na elektrické vlastnosti prvku (skratový prúd, faktor plnenia, napätie naprázdno, účinnosť, paralelné a sériové odpory) a je najvýznamnejším príspevkom degradácie.

Pre účely určovania degradačných procesov boli použité metódy ako sekundárna iónová hmotnostná spektrometria time-of-flight (TOF-SIMS), skanovacia elektrónová mikroskopia (SEM), mikroskopia atomárnych síl (AFM) a laserom indukovaný prúd (LBIC). TOF-SIMS umožňuje sledovanie degradačných procesov a zároveň vyšetovanie chemických

zmien vo fragmentoch sekundárnych iónov, sledovanie ich vývoja intenzity s hĺbkou analýzy, sledovanie interdifúzií vrstiev, ku ktorému dochádza v priebehu degradácie. Morfológia fotoaktívnej povrchovej vrstvy a jej zmena s degradáciou bola analyzovaná pomocou SEM metódy, ktorá poskytla informácie o nanoštruktúre povrchu v širokom rozsahu. Nanoštruktúra aktívnej vrstvy a jej vývoj profilu drsnosti s degradáciou bol vyšetrovaný a analyzovaný pomocou AFM. Metóda LBIC poskytla informácie o stratách elektrického výkonu prvku, ktoré nastali počas degradácie.

Táto výskumná práca určila, že degradácia organických solárnych článkov invertovanej geometrie za podmienok fotooxidácie pri laboratórnej atmosfére ovplyvňuje väčšinou materiál PEDOT: PSS a P3HT: PCBM vrstiev. Okrem toho bolo preukázané, že kyslík indukuje zmeny vlastností prvku solárneho článku, ako je napríklad oxidácia materiálov, morfológické zmeny a difúzia rozhraní, ktorá vedie k zhoršeniu vlastností súvisiacich rozhraní, a preto vedie k značnej strate napájacieho výkonu pre efektívnu konverziu. Súčasne, získané experimentálne výsledky ukazujú, že vplyv vody na štruktúru vyvoláva značnú degradáciu v organických solárnych článkoch s výrazným zhoršením vlastností zariadenia. Bolo zistené, že degradácia prebieha difúziou molekúl vody cez prvok solárneho článku, ktorá interaguje s materiálom elektród a súvisiacimi rozhraniami. Difúzia molekúl vody vedie k zmenám v podobe indukovaných nehomogenít, v ktorom pokles hustoty fotoprúdu starnutých vzoriek má následok v znížení účinnosti premeny energie. Bolo zistené, že pre dlhodobé starnutie, vyššia oxidácia fotoaktívnej vrstvy v Si-PCPDTBT: PC70BM štruktúre, by mohla viesť k vysvetleniu celkovej absencie fotovoltickej reakcie v prvku solárneho článku popísanej v literatúre. Všetky vyššie uvedené výsledky nám dávajú presnejšie vysvetlenie procesov degradácie materiálov používaných vo fotoaktívnych vrstvách v nanometrovom rozsahu. Umožňujú nám tiež lepšie pochopiť zmeny, ktoré sa vyskytujú v prvku solárneho článku počas jeho prevádzky, a eventuálne odhaliť slabé miesta organických solárnych článkov. Získané výsledky v tejto práci prispeli k pokroku v štúdií stability organických solárnych článkov.

## Abstract

In recent years, the technology of organic solar cells has become very attractive because of their advantages such as low cost processing, relative low energy polymer chemistry, flexibility, transparency and lightweight. However, intensive research is being and still need to be done in order to understand the degradation processes of used materials under standard working conditions and therefore to achieve a better stability of the devices for a large-scale application domains. The introduction of a new range of p-type polymers with a low bandgap allowed increasing the absorption of the red part of the solar spectrum and consequently the device efficiency which nowadays, is recorded above the value of 13 %. The photoactive layer is composed by a p-type polymer (electron donor molecule) blended together with an n-type (electron acceptor molecule) typically fullerene derivatives.

The materials used in the photoactive layer are not stable under standard conditions and tend to degrade as it has been shown in the literature by different research groups. The typical stress conditions that the cell is submitted to are high temperature, high/low humidity changes, ambient atmosphere, and intense light with strong UV component etc. This leads to chemical/physical degradation e.g. triplet formation from charge transfer, singlet oxygen production, oxidation of polymer, oxidation of electrodes, light assisted doping by O<sub>2</sub>, morphological changes, inter-layer reaction, delamination, diffusion of O<sub>2</sub> and H<sub>2</sub>O etc. The photoactive layer is the place where most of the listed degradation occurs and also oxygen constitutes the main reason of the device failure. In particular, the oxygen-light induced degradation known as photooxidation on the morphology parameters as well as electrical performance of the devices such as short-circuit current, fill factor, open-circuit voltage, efficiency, parallel and serial resistances, is a major contribution and require a well understanding of the processes on a nanometer scale.

For these purposes, time-of-flight secondary ion mass spectrometry (ToF-SIMS), scanning electron microscopy (SEM), atomic force microscopy (AFM) and laser beam induced current (LBIC) techniques have been applied. ToF-SIMS allows tracking the degradation processes by investigating the chemical changes on ion fragments, their intensity evolution with the depth and the inter-layer mixing that occurs during the degradation. The photoactive layer surface morphology and its evolution with the degradation were established using SEM methods, which provided information about the nanostructures

on a broad range of scales from nanometer to millimeter. The nanostructure of the active layer and its roughness profile evolution with the degradation was investigated by the means of AFM techniques. The electrical device performance (photocurrent) losses that occur with the degradation was investigated using LBIC method.

These investigations allowed to establish that the degradation of inverted geometry OSC structures at ambient atmosphere under photooxidation conditions affect mostly the PEDOT:PSS and P3HT:PCBM layer materials. Moreover, it has been shown that oxygen induces drastic changes of the device properties such as oxidation of materials, morphological changes and diffusion of interfacial layer toward semiconductors layer resulting in a deterioration of related interfaces and therefore results in a considerable loss of the device power conversion efficiency. Also, the obtained experimental results show, that water induces substantial degradation in organic solar cells with a pronounced deterioration of the device properties. It has been found that the degradation occurs by diffusion of water molecules through the solar cell device which interacts with the low work function electrodes and related interface. The water molecules diffusion leads to the observed changes in a form of induced inhomogeneities, in which the photocurrent density of the aged samples changes to a strong decrease of the power conversion efficiency. We have found that for long-term ageing, the higher oxidation of the photoactive layer as it has been observed in the Si-PCPDTBT:PC<sub>70</sub>BM blend layer structures, could be an explanation of the total absence of photovoltaic response in the cells as it has been described in the literature. All the above mentioned results give us a better understanding of the degradation processes of materials used in the photoactive layers at the nanoscale range. They allow us also to better understand the changes that occur in the PV cell during its operation and eventually figure out the device weak points. These results determine a remarkable achievements and therefore a considerable progress for the study of organic solar cells stability.



# Content

<b>I.</b>	<b>Introduction.....</b>	<b>9</b>
	I.1. Structures of Organic Solar Cells.....	10
	I.2. Materials used in Organic Solar Cells – Organic semiconductors.....	11
	I.3. Working Principle of Organic Solar Cells.....	13
	I.4. State of the Art Degradation of Organic Solar Cells.....	14
<b>II.</b>	<b>Goals of the PhD Thesis .....</b>	<b>16</b>
<b>III.</b>	<b>Experimental Methods.....</b>	<b>18</b>
<b>IV.</b>	<b>Photooxidation of P3HT:PC60BM.....</b>	<b>19</b>
	IV.1. Introduction .....	19
	IV.2. Results and discussion.....	19
<b>V.</b>	<b>Photooxidation of Si-PCPDTBT:PC70BM.....</b>	<b>22</b>
	V.1. Introduction .....	22
	V.2. Results and discussion.....	23
<b>VI.</b>	<b>Damp-heat of P3HT:PC60BM.....</b>	<b>27</b>
	VI.1. Introduction.....	27
	VI.2. Results and discussion.....	28
	VI.2.1. <i>j</i> - <i>V</i> curves of degraded multi-layers structures.....	28
	VI.2.2. Degradation of single layers structures.....	31
<b>VII.</b>	<b>Summary and Conclusion.....</b>	<b>32</b>
	<b>References.....</b>	<b>37</b>
	<b>List of publications.....</b>	<b>39</b>

# I. Introduction

Alternate and renewable energy sources became much more attractive compare to traditional fossil fuels which in addition for being non-renewable, are harmful toward the environment and causes change in climate as global warming. Among the renewable energy sources that include sunlight, water, wind and geothermal heat, photovoltaics since 2004, has attracted the industry of energy technology principally due to the decreasing cost of installation as it has been reported by the Lawrence Berkeley National Laboratory. The term photovoltaic means production of energy from natural light. Put another way, the energy of the photons that compose the sunlight is converted to electrical energy following the photovoltaic and conversion reactions. It has been found out that the production of energy through photovoltaic conversion has been increased by an average of more than 20% each year [1].

Many experiments have documented the photovoltaic effect; however, the most known example is the one of Becquerel [2] which is actually considered as the first proof of photovoltaic principle. However, in the early of 1950s, the photovoltaics developed into the more useful form of solar cell as we know them today by the implementation of the bulk semiconductors. The first solar cell, based on diffused silicon, has been made by Daryl Chapin, Calvin Souther Fuller and Gerald Pearson [3] and shortly thereafter, many applications have been envisaged. The advantages of the organic materials for photovoltaics compared to inorganic materials as silicon are:

- Low cost processing,
- Relatively low energy polymer chemistry,
- Flexibility (roll to roll processing),
- Transparency and,
- Lightweight.

Shirakawa et al., in 1977 published a paper based on the synthesis of electrically conducting organic polymer [4]. In 2000, Alan Heeger, Alan MacDiarmid and Hideki Shirakawa have been awarded the Nobel Prize for discovering organic photovoltaics. The efficiency reported from those organic solar cells was approximately fourth times below the

efficiency of inorganic cells ones. However, other than ensuring high efficiency and low cost manufacturing for organic solar cell devices, another important challenge is to ensure their stability and therefore prevent their degradation at standard condition, mostly in air [5–9].

David L. Staebler and Christopher R. Wronski observed in the early of 1977 a rapid decrease in the performance of silicon solar cell under illumination mostly known as the Staebler-Wronski effect [10]. This has been the starting point of the degradation investigation that occurs in solar cells. The early reports on degradation of organic solar cell devices started appearing at 1990 approximately [11]. Thereafter, various techniques have been applied in order to study the degradation process that occurs in solar cells which depend to the environment in which the cells are kept. In a book that summarizes the state of the art understanding of stability and provides a detailed analysis of the mechanism by which degradation occurs, Krebs et al. [12] report the complexity of the degradation process and the enormously variables in all aspects that polymer solar cells present.

## I.1 Structures of Organic Solar Cells

While inorganic semiconductors electronic devices are generally composed of p-n heterostructures, in organic semiconductors devices, heterojunctions formed by two different materials are used in the active layer. Two main types of organic heterojunctions structures can be distinguished:

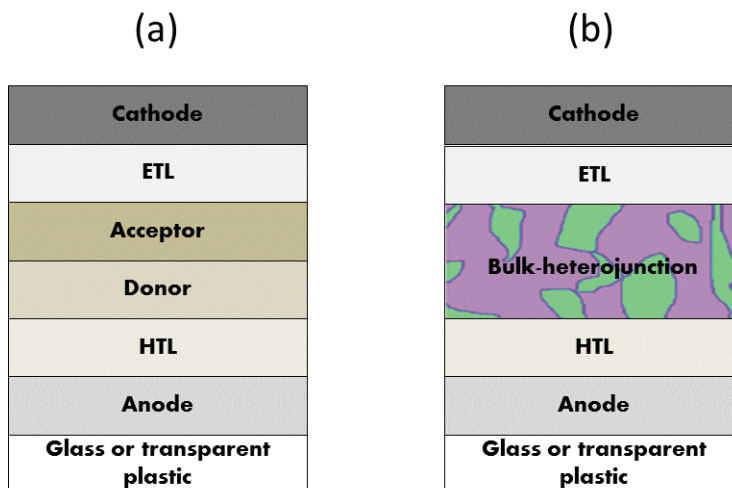


Figure 1.1. Schematic diagrams of a planar (a) and a bulk-heterojunction (b) structures organic solar cell. ETL and HTL are electron transport layer and hole transport layers respectively.

- Planar heterojunctions formed by multilayer structures (Figure 1.1.a) are fabricated by vacuum depositing of successive small molecule layers, or by processing from polymer solution or small molecule layers [13].
- Three dimensional diffused heterostructures (Figure 1.1.b) often called bulk heterojunctions (BHJ) are obtained by blending two or more materials in common solvents.

The bulk-heterojunction compared to planar heterojunction takes advantage of the most unique property of organic semiconductors that is their solubility and thus open the possibility for production of new solid composites with specific physical properties without the need of synthesizing new materials. Also, by mixing of a p-type and n-type semiconductors together enables active layers to show ambipolar transport characteristics since for instance, organic materials usually show unipolar charge transport where holes and electrons are the dominant charge carriers.

Moreover, in photovoltaic, bulk heterojunctions structure are preferred over the single layer since a good charge mobility (electron and hole) are needed for an efficient charge separation and conduction toward the electrodes [14]. Organic solar cells can be categorized as conventional (standard) or inverted according to which side is the closest to the substrate. In the conventional OSCs, the anode is directly deposited onto substrate, while in the inverted; the cathode is directly deposited onto the substrate. Despite the different structure that OSCs can have, the working principle remains the same.

## **I.2 Materials used in OSCs – Organic semiconductors**

The term organic is employed when dealing with carbon-based materials as polymers for example. A semiconductor is a material that possess a gap energy  $\Delta E$  (generally in the range between 1.5 – 3 eV [15]) defined as the energy value between the valence (highest occupied molecular orbital or HOMO) and the conduction (lowest unoccupied molecular orbital or LUMO) bands. Therefore organic semiconductors define a large family of organic materials that shows semiconducting properties. Two main groups of organic semiconductors can be distinguished: low molecular weight materials also called oligomers and polymers. Both groups have a common characteristics which is the arrangement of the carbon atoms in a series of alternating single and double bonds mainly known as conjugation.

In the state of the art of OSCs technology, P3HT as p-type (electron donor) polymer and PCBM as n-type (electron acceptor) are the two most widely used materials and have been the subject of numerous studies [16–18]. However, compared to fullerenes, PCBM is a more practical choice for an electron acceptor due to its good solubility in mostly used solvents such as chlorobenzene, dichlorobenzene etc.[19]. The solubility is a necessary property for solar cells as it allows the solution processable donor/acceptor mixes.

However, many others p-type polymers as poly[2,6-(4,4-bis-(2-ethylhexyl)-4H-cyclopenta[2,1-b:3,4-b']dithiophene)-alt-4,7-(2,1,3-benzothiadiazole)] (PCPDTBT), poly[2,6-(4,4-bis-(2-ethylhexyl)dithieno[3,2-b:2',3'-d]silole)-alt-4,7-(2,1,3-benzothiadiazole)] (Si-PCPDTBT) and poly [(4,4' – bis (2-ethylhexyl) dithieno [3,2-b:2',3'-d] silole) -2,6-diyl-alt-(2,5-bis 3-tetradecylthiophen-2-ylthiazolo 5,4-d thiazole)-2,5 diyl] (EP10) emerged progressively. These polymers possess interesting optical properties especially toward light absorption due to their low band gap which allows extending the absorption proportion on the solar spectrum. At the stage of laboratory research, the silole-based polymer EP10 is beginning to receive considerable attention. The devices made with EP10:PC<sub>70</sub>BM materials show a power conversion efficiency of 5% [20–22]. The chemical structures of the above cited polymers are presented in Figure 1.2.

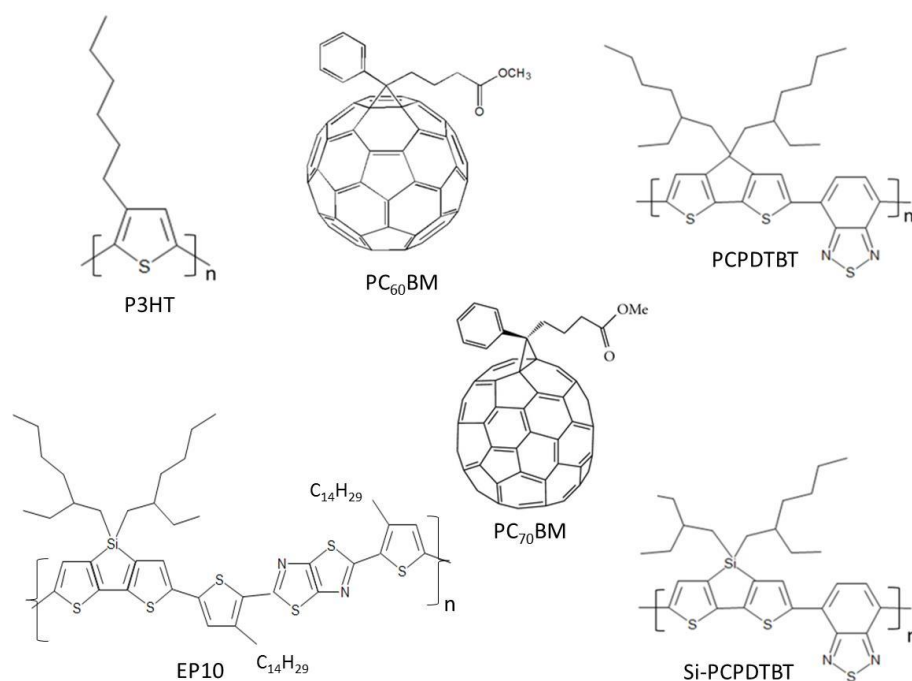


Figure 1.2. Chemical structures of P3HT, PCPDTBT, Si-PCPDTBT, EP10, PC<sub>60</sub>BM and PC<sub>70</sub>BM materials.

### I.3 Working Principle of Organic Solar Cells

A single-junction organic solar cell comprises five to six layers stacked on a supporting substrate as shown in Figure 1.3 a.

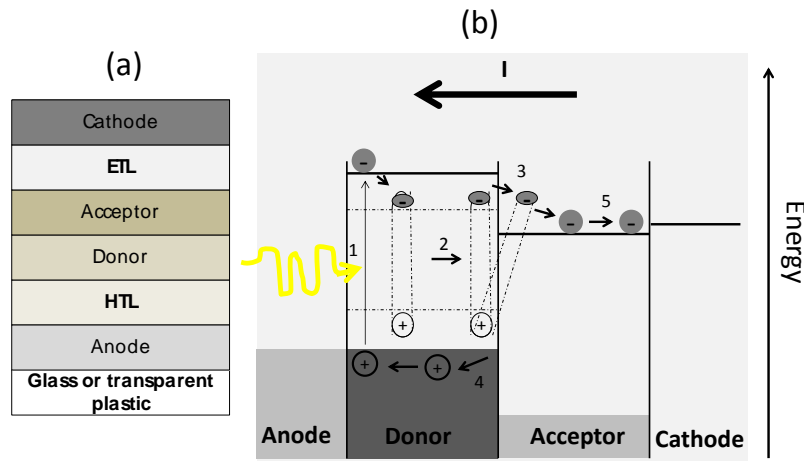


Figure 1.3. Schematic view of OSCs (a) and the working principle of OSCs with production steps of electrical in an organic solar cell (b) [23].

The different layers that constitute single-junction organic solar cells are:

- A photoactive layer: It is the principal part of the device as there will be the charge carriers generated when the device is submitted to illumination. It is composed of two materials, a p-type polymer (electron donor) blended with an n-type (electron acceptor).
- Electrodes: An anode and a cathode are used as electrodes. One of them has to be transparent so that the light can reach the photoactive layer. Mostly, indium-tin-oxide (ITO) is used as transparent electrode and the other electrode is made from aluminium or silver.
- Transporting layers: In a real OSC device, additional specific layers are used in order to improve charges (hole in the donor and electron in the acceptor) transport toward the electrodes. Usually zinc oxide (ZnO) or titanium oxide (TiO<sub>2</sub>) layers due to their good conductivity and transparency are used as electron transporting layer (ETL), and poly(3,4-ethylenedioxythiophene)-compl-poly(styrenesulfonate) (PEDOT:PSS) as hole transporting layer (HTL).
- Substrate: Usually, glass or plastic foils are used as support. This later one awards to the device high adaptability to diverse areas as it is flexible.

Sometimes, an extra encapsulation film is employed. Contrarily to the inorganic solar cells where the charges carriers are generate directly by the light absorption inside the bulk of the intrinsic layer, in organic solar cells, the absorption of light generates a neutral excited state called exciton. The production of electrical energy in an organic solar cell includes five sequential steps as shown in Figure 1.3 b [23]. The absorption of a photon in the photoactive layer results in an electron excitation from the HOMO to the LUMO of the electron donor material forming tightly-bound exciton (electron-hole pair). Once the exciton is created, it diffuses inside the electron donor material to the interface electron donor – acceptor materials. The dissociation of the exciton at the interface between the donor and acceptor materials yields mobile charges (hole and electron). The electron goes to the cathode and the hole to the anode. The dissociation of the exciton is achieved because of the difference of the work function of the electron donor and acceptor materials which is greater than the binding energy of the excitons.

#### **I.4 State of the Art Degradation of Organic Solar Cells**

Although the fact that organic photovoltaics (OPV) has become one of the most studied domains in the field of renewable energy sources, progress concerning the stability of the used materials needs to be achieved. Indeed, the used materials are unstable and tends to degrade at standard conditions namely ambient atmosphere and sun-illumination following different process that are either, reversible upon annealing under vacuum/nitrogen atmosphere or irreversible. Depending on the significance of air exposure, the degradation of OSCs can be divided into intrinsic or extrinsic. The first one is caused by the thermal interdiffusion of constituent species inside the OSCs, while the latter is caused by the intrusion of external constituents as air or water [24]. Both types of the above mentioned degradation are mass-transport process (diffusion). Before we go into the deep and comprehensive analysis of this topic, it has to be mentioned that OPV presents a very complex selection of degradation phenomena [25].

Moreover, even if the efficiency at the region of 5 up to 12 % [26–27] on 1x1 cm<sup>2</sup> size area is currently approaching the efficiencies of inorganic silicon-based solar cell technology, which is readily available at large scales and works with quite good efficiencies (of the order of 24%) and lifetimes around 25 years [28], the OSCs must be improved to become industrially interesting for large scales. For this, the fast efficiency losses present in many high efficiency materials will need to be sorted out [29]. The stability, the efficiency and the

process of the device manufacturing are linked together (Figure 1.4), and nowadays the combination of these three properties has only been attempted in a few reports [30–31].

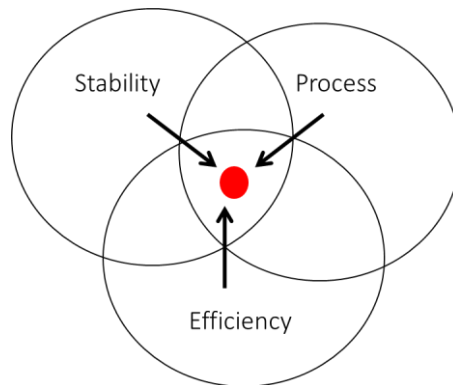


Figure 1.4. Challenge of the efficiency, stability and process for the same material.

Exposed to sunlight, organic materials react via photochemical reactions that are affected by the presence of component in atmosphere e.g. oxygen, water and leads therefore to the device failure. As previously mentioned, the degradation process of OSCs is very complex with many types of chemical and physical degradation e.g. polymer oxidation, electrodes oxidation, morphological changes, inter-layer reaction, delamination, oxygen and water adsorption and diffusion etc. However, concerning the interfaces degradation, it has been shown by Reese et al. [32] that the metal-organic interfaces are where the major degradation takes place, even if the OSCs are stored in an inert atmosphere. Figure 1.5 summarizes the different types of degradation that can happen to the device and lead therefore to its failure [5].

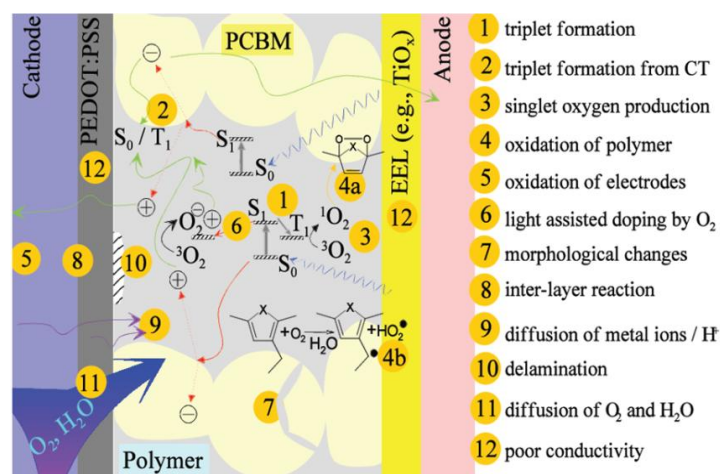


Figure 1.5. Cross section view of a solar cell device with typical degradation processes that can take place in a bulk heterojunction and leads to decrease in efficiency [5].

## II. Goals of the PhD Thesis

As described in the paragraph *I.5 State of the Art Degradation of Organic Solar Cells*, it is clear that the degradation of OSCs is a tricky process that needs more and more investigation. To investigate such a phenomena the use of multiple and diverse characterization techniques that provide complementary information become crucial. This thesis deals with the study for a better understanding of the degradation processes that impact OSC materials and leads to the device failure. The main objectives will be to elucidate and go beyond the state-of-the-art in order to understand the degradation mechanisms of OSCs and thus deliver information on the degradation between two layers in OSCs. The motivation is that ageing induces chemical modifications of used materials which impair the OSCs performance. Thus, a detailed relationship between chemical degradation at nano and macro-morphologies and the device performances is needed. The work will be centered to an elucidation of organic-materials degradation mechanisms under different conditions (photooxidation, damp-heat and photolysis) based on the chemical evolution of the bulk heterojunction (BHJ) layer, the surfaces and interfacial layer ageing where the objective will be to relate ageing and surface effects to nano-scaled interfacial variations. Another motivation is that the prime cause of short OSCs lifetimes is layer delamination. The nano-morphology stabilization and the evolution of BHJ blend layers with an objective to deliver an insight view to the BHJ morphology, its evolution with ageing and effect on material-related electrical properties would be explored. A stable morphology is pivotal to stable OSCs, once it is established that the morphology has the domain-scale to enable charge formation and percolation.

The objectives of this thesis can be summarized by the following points:

- To investigate and explain the degradation mechanisms of OSCs with diverse characterization techniques, which provide complementary information.
- To provide a detailed investigation of relationship between chemical degradation at nano and macro-morphologies and eventually correlate them with the device performance loss.

- To elucidate the degradation mechanisms of organic-material under different condition (photooxidation, damp-heat and photolysis) based on the chemical evolution of the bulk heterojunction layer, the surfaces and interfacial layer ageing and to relate ageing and surface effects to nano-scaled interfacial variations.

To achieve these goals, different analytical methods based on chemical method as time-of-flight secondary ions mass spectrometry (ToF-SIMS) and physical methods as laser beam induced current (LBIC), scanning electron microscopy (SEM) and atomic force microscopy (AFM) will be applied. As shown in the literature [9, 12, 17, 35, 36–37], the use of those techniques provide crucial information that allows tracking the degradation process of OSCs in order to better understand it's mechanism and therefore propose strategic routes for a better stability of the device.

ToF-SIMS has been used in OPV technology to study the degradation process due to his ability to provide chemical information which can allow tracking the degradation process. SIMS can provide mass spectra analysis which allows determining the elemental and molecular species on a surface. Scanning the ion beam over a surface area provides an ion image of any given mass spectra marker (i.e. any surface species). A depth profile is constructed from a stack of ion images as a function of depth. A probe depth of the primary analysis ion of only 1-2 nm combined with the ability to obtain ion images as a function of depth enables specific OPV layers to be analyzed i.e. degradation can be monitored or detected in any given point in the OPV device including interfaces [12].

Due to his advantages such as superior lateral resolution and the capability to analyze a broad range of scales from nanometer to millimeter range, SEM has become a standard tool for visualizing morphology in OPV technology. SEM is used in OPV in order to visualize and optimize materials nanostructures allowing thus the optimization of OPV efficiency [35]. SEM also allows imaging by cross-sectional analysis which is very useful when investigating interface nature in OPV.

The main use of AFM in OPV has been focused on characterization of the nanostructure in the bulk heterojunction active layer depending on the solvent choice, annealing method; blend ratios etc., in order to optimize the device efficiency [34]. The contribution of AFM to study the stability and degradation of OPV has been typically limited to support conclusions obtained using other methods [12]. AFM allows the acquisition of topography images with an excellent lateral resolution and an excellent height resolution both

at Angstrom range as well as phase images that visualize contrast in physical properties on the surface which may allow visualizing the chemical contrast in some cases [12].

Laser beam induced current (LBIC) is an optical technique that is used to analyze semiconductor material properties. Studied aimed to track the degradation in OSCs has been realized by different groups using LBIC method [38]. Recently, LBIC has been used for lateral characterization of organic solar cells device performance by a mapping of the photocurrent [39–41].

### III. Experimental Methods

Ion-ToF (SIMS IV) in dual beam mode was used to perform chemical depth profiling measurements. A liquid metal ion gun  $\text{Bi}^+$  at 25 keV was used as analyzer gun and  $\text{Cs}^+$  at 1 keV as sputtering gun with  $300 \mu\text{m} \times 300 \mu\text{m}$  size of the scanned area. Different measurement conditions e.g. different  $\text{Cs}^+$  energy (from 1 to 2 keV), flood gun etc. were tested in order to minimize the measurement uncertainty. Scanning probe microscope (Solver P47H-PRO) was used for AFM measurement in semi-contact mode to characterize the surface properties. The measurements were done on different areas ranging from  $2 \times 2 \mu\text{m}^2$  to  $5 \times 5 \mu\text{m}^2$  ( $256 \times 256$  points). SEM LEO 1550 equipped with In-Lens and Everhart-Thomley (SE2) secondary electron detectors was also used to characterize the surface morphology of Si-PCPDTBT:PC<sub>70</sub>BM blend layers. The energy of the electron beam was set to 5 keV but other energies were tested also to achieve optimal contrast and lateral resolution. Also, different size areas, from nanometer (nm) to millimeter (mm) range were investigated. Current-voltage characteristics (I-V curves) of solar cells devices were measured under the dark conditions and by illumination under the Steuernagel solar simulator in nitrogen atmosphere at intensities of 80 or 100  $\text{mW}/\text{cm}^2$ . The illumination of the cell has been performed from the glass side. Main device parameters including open circuit voltage ( $V_{oc}$ ), electrical fill factor ( $FF$ ), power conversion efficiency ( $\eta$ ) and short-circuit current density ( $J_{sc}$ ) as well as the current density-voltage ( $j$ -V) curve were calculated from measured I-V curves.

## **IV. Photooxidation of P3HT:PC60BM**

### **IV.1. Introduction**

This chapter is focusing on the study of the degradation effect of inverted geometry organic solar cell devices consisting of PEDOT:PSS/P3HT:PCBM/ZnO/ITO, where PEDOT:PSS is the poly(3,4-ethylenedioxythiophene) polystyrene sulfonate. The layers were deposited on precoated ITO/glass substrate. The structures were degraded for 10, 30, 60 and 120 min by exposing to the ambient atmosphere illuminated under the sun simulator (AM 1.5G). Inverted geometry OSCs is preferred to a normal geometry OSC because it appears more stable at ambient atmosphere as it were investigated by Norrman et al [9]. Time-of-flight secondary ions mass spectrometry (ToF-SIMS) depth profiling was used to investigate the chemical modifications of the materials in the device structure. The surface morphology changes that occurs on the top layer (PEDOT:PSS) were characterized using scanning electron microscopy (SEM), atomic force microscopy (AFM) and optical microscopy (OM) methods. The results obtained using the above specified methods are presented and discussed successively in the next paragraphs.

### **IV.2. Results and Discussion**

SEM images (Figure 4.1) were acquired on the PEDOT:PSS surface in order to get more information about the evolution of this layer during the degradation process. The images show a presence of defects (holes and hills) on top layers of the non-degraded and degraded samples. The holes presented on the surface are shown at high magnification in Figure 4.1A. It has been found, that the degradation process does not contribute to the density of holes indicating that holes in the PEDOT:PSS are related to deposition process rather than to degradation itself. On the other hand, defects on the PEDOT:PSS surface decorated by “white spots” or “white structures” of various size and shape (see e.g. Figure 4.1C) have evolved on samples degraded for 60 and 120 min. The white contrast in secondary electron images detected by InLens detector could be correlated to chemical changes in the PEDOT:PSS, but the nature and composition needs further detailed investigations.

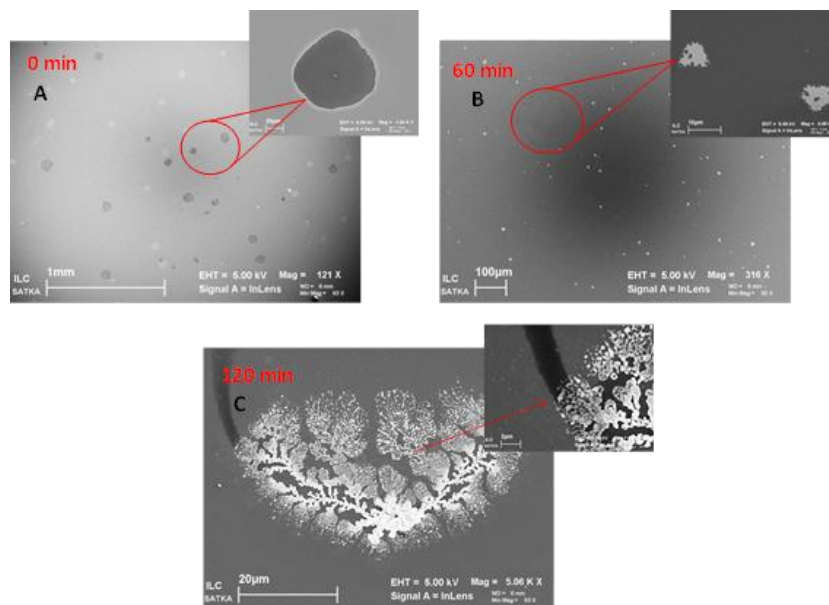


Figure 4.1. SEM images of the PEDOT: PSS layer: (A) non-degraded, (B) degraded for 60 min and (C) degraded for 120 min.

Also, the effect of the SEM electron beam to the organic materials layer properties has been investigated. For this purpose, SEM images of a virgin surface (Figure 4.2A) and a surface after 30 minutes (Figure 4.2B) of P3HT:PCBM surface layer have been recorded under vacuum with electron beam. An appearance of “new” structure is clearly seen exactly at the location, from which the SEM was taken and the electron beam was rastered (Figure 4.2B). These results lead us to the fact that chemical changes are induced during the sample measurement using SEM method. Indeed, Krebs et al [43] also described that the electron beam of a SEM is highly energetic and even could thus degrade the organic components by inducing morphological changes in the OPV device, which would complicate the interpretation of subsequent analysis data.

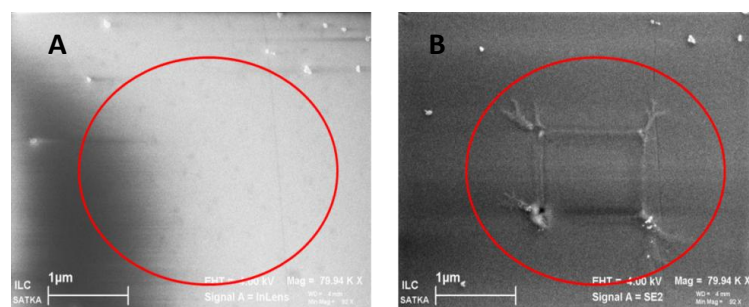
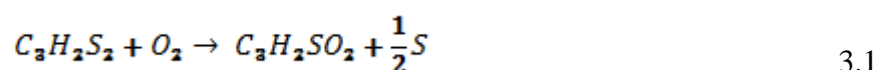


Figure 4.2. SEM SE images of P3HT:PCBM surface layer under vacuum with electron beam: simultaneous image (A) and image after 30 seconds (B).

ToF-SIMS depth profiles of the non-degraded and degraded structures (not shown here) show no remarkable change in the yield of different ion fragments. Due to the fact, that no degradation was seen from the ion fragment profiles, we decided to investigate the overall SIMS spectra of the structure, related to the chemical changes of materials due to the degradation. Figure 4.3 shows the evolution of selected target ions peaks obtained from the spectra of non-degraded structure and degraded for different time (30 min, 60 min and 120 min). In Figure 4.3A, the peak at 101.92 u.a, attributed to the  $C_3H_2S_2$  ion fragment (as a part of P3HT) decrease at intensity with the degradation time. Proportionally to the decreasing of  $C_3H_2S_2$  peak intensity, another peak attributed to  $C_3H_2SO_2$  appears at 101.94 u.a. We suppose that this results from the oxidation by atmospheric oxygen which could be illustrated by the following reaction (3.1):



The peak located at 73.93 u.a in Figure 4.3B is attributed to a  $C_3H_6S$  coming the most probably from the P3HT material.

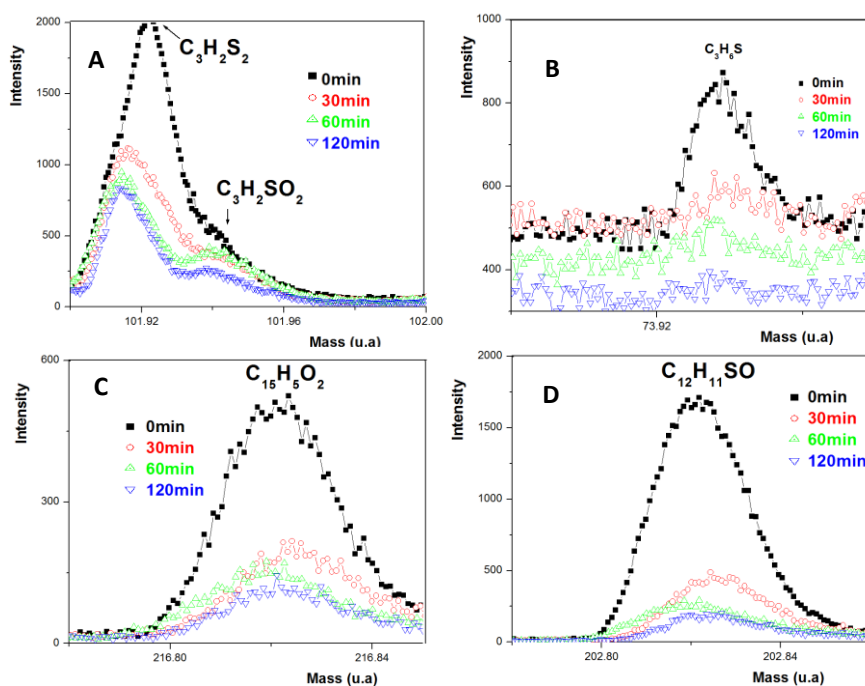


Figure 4.3. Depth-integrated ToF-SIMS spectra of inverted geometry OSC structures degraded for 0, 30, 60 and 120 min.

After the 120 min degradation, this peak disappeared which is probably due to the effect of the degradation. The peak located at 216.82 u.a in Figure 4.3C, attributed to the  $C_{15}H_5O_2$  ion fragment shows his intensity to decrease strongly and progressively with the degradation time. This ion fragment may come from the PEDOT:PSS or PCBM. The decreasing intensity with the time provides evidence of the chemical effect of the degradation. The peak located at 202.82 u.a in Figure 4.3D, associated to  $C_{12}H_{11}SO$  ion fragment also shows a strong intensity decreasing with the degradation time linked to the degradation. This peak we suppose originate from the PEDOT:PSS material and not from oxidized P3HT the peak was well present with the highest intensity at the undegraded sample.

## V. Photooxidation of Si-PCPDTBT:PC70BM

### V.1. Introduction

Another promising low bandgap material is the silicon-bridged Poly[2,6-(4,4-bis(2-ethylhexyl)dithieno[3,2-b:2,3-d]silole)-*alt*-4,7-(2,1,3 benzothiadiazole)] or Si-PCPDTBT (Figure 5.1b) whose energy bandgap below 1.4 eV is well suited for the use as electron donor polymer in bulk heterojunction solar cells [44–48]. Scharber et al. [49] showed by replacing the bridging carbon atom in the cyclopentadithiophene by a silicon atom that a higher crystallinity, an improved charge transport properties, a reduced bimolecular recombination and also formation of charge transfer complexes can be achieved when blended with a fullerene. This replacement introduces a small distortion of the cyclopentadithiophene unit of the polymer. Indeed, the Si-C bond is longer than C-C and modifies the geometry of the fused dithiophene unit which is enough to achieve a better ordering of the polymer chains leading to the improvement listed above. Also, one needs to mention that Si-PCPDTBT was the first low-bandgap polymer to have a certified efficiency of over 5%. Manceau et al. [50] showed that the key step of the P3HT degradation mechanism is the H-abstraction in the alkyl side chain at the alpha position of the thiophene ring. This problem is not encountered in the case of PCPDTBT and Si-PCPDTBT polymers, where this position is protected by the alkyl chains. The alkyl chains protect the alpha position against oxygen attack which thereby makes these polymers more stable against oxidation.

The schematic cross-section of the investigated structures as well as the chemical structure of fullerene derivative PC70BM are given in the Figure 5.1. Recent studies of the

state of the art system P3HT:PC<sub>60</sub>PM using SIMS by the Krebs group [9, 29] has shown that this method provides valuable information in this context.

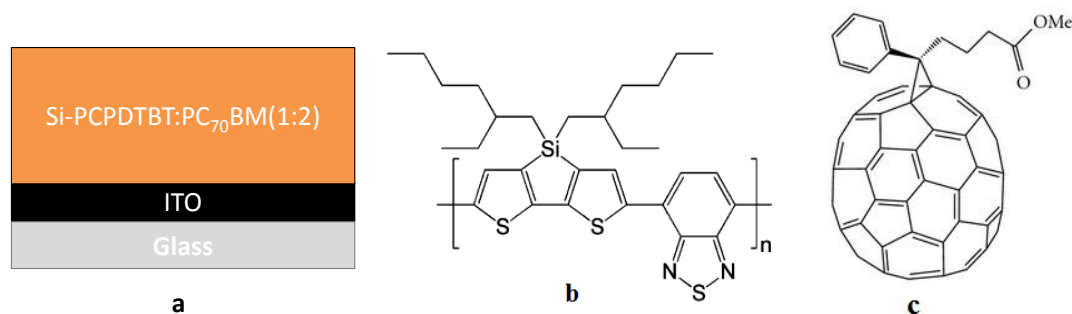


Figure 5.1. Schematic cross-section of the investigated structures (a), and chemical structure of the Si-PCPDTBT (b) and PC<sub>70</sub>BM (c) materials.

## V.2. Results and discussion

SIMS depth profiles of the unexposed and differently photooxidized Si-PCPDTBT:PC<sub>70</sub>BM blend layers are shown in the Figure 5.2. The top left figure displays ion depth profiles recorded from a non-degraded active blend layer. The O<sup>-</sup> ion fragment intensity and those of oxidized layer species demonstrate the presence of oxygen in the layer. The profiles appear rather flat over the film thickness in this manner suggesting homogeneous distribution of those species. Decrease of carbon and increase of InO<sup>-</sup> and even O<sup>-</sup> ion fragments indicate the position of the interface to the ITO substrate. Following the first photodegradation step (30% UV loss, see Figure 5.2, top right) a significant increase of the oxygen and of the NO<sup>-</sup>, NO<sub>2</sub><sup>-</sup>, SO<sup>-</sup>, SO<sub>2</sub><sup>-</sup>, CO<sup>-</sup> ion fragment intensities becomes evident, which is caused by the oxygen diffusion and photooxidation of the active polymer material (Si-PCPDTBT: PC<sub>70</sub>BM).

However, the oxygen ion and oxidized ion fragment intensities are not constant anymore with depth, but decay from significantly enhanced intensities close to the film surface to intensities similar to those in the as prepared reference non degraded active layer blend close to the buried interface to ITO. This is clear evidence for an inhomogeneous distribution of the oxidized species with an enhancement (only slightly less than an order of magnitude) near the surface. Photooxidation proceeds faster closer to the surface compared to the buried interface. At least part of the concentration gradient of the oxidized species with depth can be related to the expected exponential decrease of the light intensity, which is

needed to drive the photooxidation of the light absorbing film, with depth distribution described by the Lambert-Beer absorption law.

In addition, an even stronger intensity enhancement very close to the film surface may be recognized for the less oxidized ion species ( $\text{SO}^-$ ,  $\text{NO}^-$ ) compared to the higher oxidized ions ( $\text{SO}_2^-$ ,  $\text{NO}_2^-$ ) ions. In contrast, the oxygen-free  $\text{C}_3^-$  ion fragment exhibit about similar intensities for both samples and does not indicate inhomogeneity. Interestingly, the  $\text{SiO}^-$  ion fragment does not increase significantly in intensity after the first photodegradation step and indicates almost homogeneous  $\text{SiO}^-$  distribution. These observations are in line with suggestions that traces of inactive inorganic Si oxide species are present in the matrix of the organic active blend layer, which determine the observed  $\text{SiO}^-$  ion fragment intensity mostly.

In the bottom of Figure 5.2 ion depth profiles are provided for the two highest degree of photodegradation (62% and 77% UV loss). The intensities of the oxidized ion species appear again increased further all over the depth of the film compared to the former degradation step. In addition, the surface enhancement of some of the less strongly oxidized ion species ( $\text{SO}^-$ ,  $\text{NO}^-$ ) becomes even more pronounced. The apparent sputtering time of the near-surface region with significantly enhanced intensities of such species becomes about 200-300 seconds in interesting correlation to the apparent sputtering time of reduced  $\text{C}_3^-$  ion fragment intensities. At present, the reason for the evidently enhanced near surface photooxidation is not clear yet, but the effect observed with ToF-SIMS here seems to fit to other our unpublished XPS experimental results.

The sputtering time till arriving at the ITO interface becomes significantly reduced with increasing photooxidation which may be related to modification of sputtering rates with oxidation and/or loss of material due to the desorption of volatile oxidation products. Indeed, previous studies revealed that photooxidation of organic materials can be manifested by a formation of low weight photoproducts in gas phase due to the presence of holes and erosion [150].

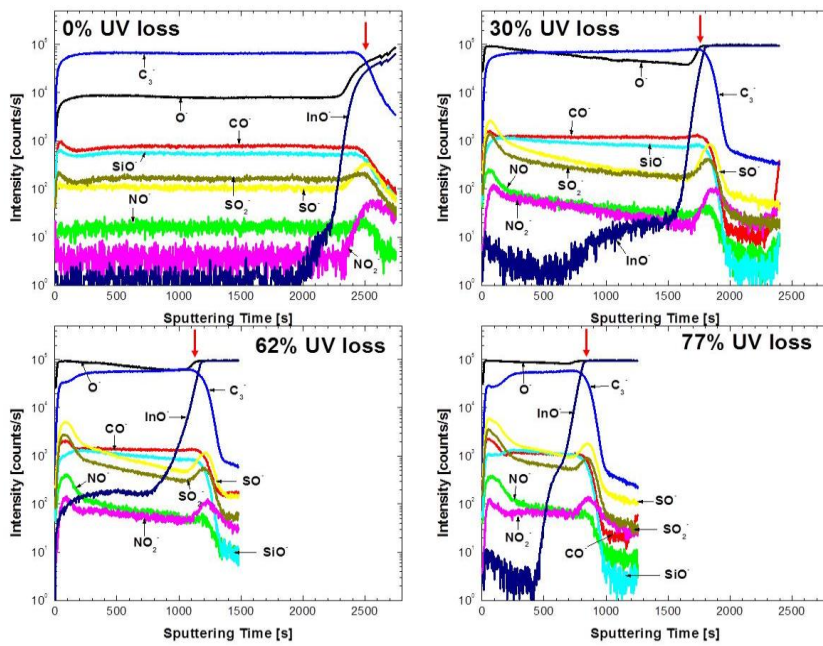


Figure 5.2. ToF-SIMS depth profiles of Si-PCPDTBT:PC<sub>70</sub>BM/ITO/glass at different levels of photooxidation (0%, 30%, 62% and 77% of UV absorbance loss). The interface of the Si-PCPDTBT:PC<sub>70</sub>BM and ITO layer is identified by the red arrows in the figures.

AFM and SEM techniques were applied in order to characterize the behavior of the sample surface morphology according to the photooxidation steps.

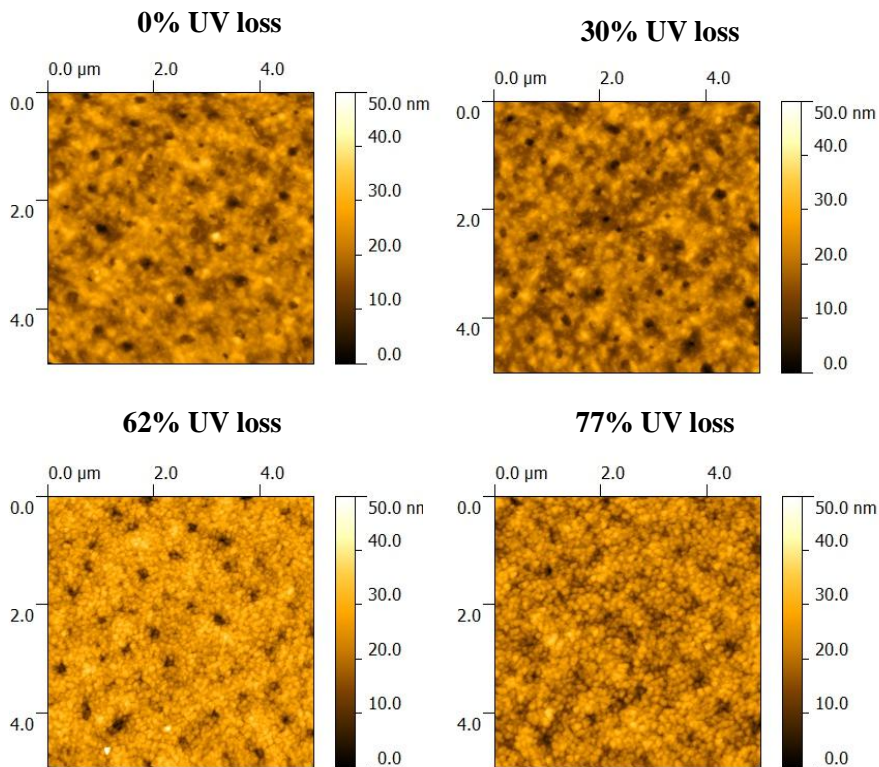


Figure 5.3. AFM images of Si-PCPDTBT:PC<sub>70</sub>BM blend layers before (0%), and after different levels of degradation (30%, 62% and 77% of UV absorbance loss).

The AFM surface morphology images presented in Figure 5.3 reveal good uniformity of the layers surface, preserved also after the photoaging resulting in 77% UV loss. This is reflected in small variation observed on the roughness parameters ( $R_a$ , RMS) (not shown here). The  $R_a$  and RMS values before and after photoaging appears very similar. The observed variation from 0.1 to 1 nm increases after 30% of UV absorbance loss before to keep decreasing with the % of UV absorbance loss. After 77% UV absorbance loss, the obtained  $R_a$  and RMS values are almost the same to the ones before degradation. Also visible are the “holes” on the surface of the layers, with not clearly defined periodicity. Moreover, Seo et al. [52] found in their study a surface relatively smooth and homogenous of the Si-PCPDTBT:PC<sub>70</sub>BM blend layer (deposited on silicon substrate) which they ascribed to an indication of a well intermixed bulk of Si-PCPDTBT and PC<sub>70</sub>BM materials.

SEM was applied in order to get complementary information about surface changes according to the degradation. The different SEM images of the surface obtained at varied steps of degradation (% UV absorbance loss) are presented in Figure 5.4. They reveal flat surface of the unexposed layer, with morphology features very similar to that observed in AFM images. Rarely, some clusters of the organic material were found on the surface (e.g. marked in Figure 5.4a). However, nano-objects homogeneously dispersed over the layer surface were observed on degraded samples. On the most degraded layer, the objects (white in the SEM image) have a clear fibril form lying on the layer surface.

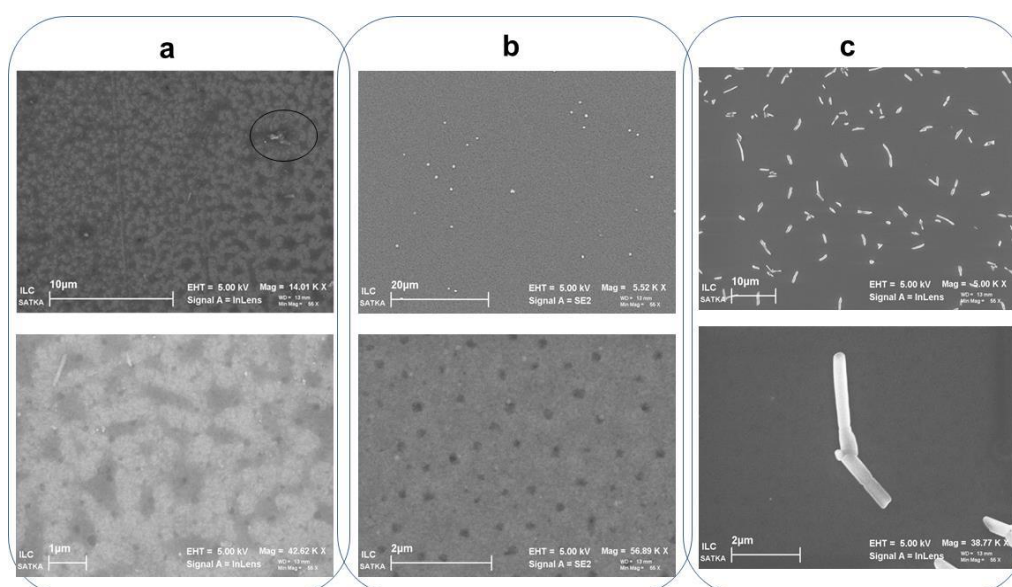


Figure 5.4. SEM images of Si-PCPDTBT:PC<sub>70</sub>BM blend layers before 0% (a), and after degradation 30% of UV absorbance loss (b) and 77% of UV absorbance loss (c).

From the initial part of the SIMS depth profiles in Figure 5.2 (around 200-300 s from the surface) it is evident that the photoassisted degradation leads to significant increase of the ions fragments content especially in the upper part of the layers. Correlating the results obtained by SEM methods with SIMS depth profiles it is evident, that the photoassisted degradation in ambient air results in a diffusion of oxygen and other gaseous molecules into the photoactive layer. The process is accelerated by the layer oxidation and volatilization seen from the carbon profiles and AFM morphology. The oxidation of the layer surface and formation of the nano-objects may also explain the layer morphology changes during the degradation.

## VI. Damp-heat of P3HT:PC60BM

### VI.1. Introduction

In this study, a setup has been designed and built specifically for damp heat degradation. With this setup the effect of water on solar cell devices, with a structure of glass/ITO/PEDOT:PSS/P3HT:PC<sub>60</sub>BM (1:0.7)/LiF/Al, has been investigated. The effect on characteristic device parameters like opens-circuit voltage ( $V_{oc}$ ), fill factor (FF), power-conversion efficiency ( $\eta$ ) and short circuit-current ( $J_{sc}$ ) as well as the current density-voltage curves ( $jV$ ) have been investigated. Laser beam induced current (LBIC) has been applied as a complementary technique in order to acquire more information about the degradation that occurs in the device. Two experiments, a single-layer and a multi-layer degradation have been performed. Figure 6.1 summarizes the description of the different experiments.

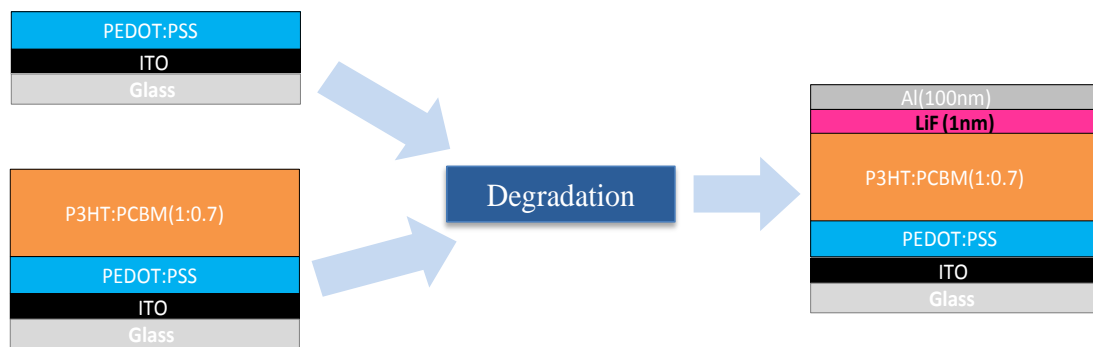


Figure 6.1. Damp heat degradation experiment with single and multi-layer structures of solar cells.

- i. Single-layer degradation: In this experiment the PEDOT:PSS layer deposited on precoated ITO/glass substrate is degraded first, then the photoactive layer P3HT:PC<sub>60</sub>BM(1:0.7), the hole blocking layer (LiF) and finally the top electrode (Al) are deposited in order to finish the device.
- ii. Multi-layer degradation: In this experiment, a multi-layer structures consisting of glass/ITO/PEDOT:PSS/P3HT:PC<sub>60</sub>BM(1:0.7) is degraded first, and then the device is finished by evaporating the LiF and Al layers.

## VI.2. Results and discussion

### VI.2.1. *j*-*V* curves of degraded multi-layer structures

The degradation experiments with the multi-layer, glass/ITO/PEDOT:PSS/P3HT:PC<sub>60</sub>BM (1:0.7) structures were performed over a time period of 10 hours. The obtained results are summarized in Figure 6.2. In Figure 6.2A  $V_{oc}$  and  $J_{sc}$  are plotted versus degradation time. The  $V_{oc}$  is stable with degradation time, only a drop of 10% is measured after 10 hours of degradation. This may be attributed to a “soaking” of the cell. The  $J_{sc}$  shows a degradation trend with a progressive decrease versus the degradation time. Almost 77% loss of the initial  $J_{sc}$  is observed after 3 hours of degradation. After 10 hours, only 24% of the initial value remained.

The evolution of the FF and Eff are plotted in Figure 6.2B. A progressive decrease of the FF is observed versus degradation time. After 10 hours, the initial value has decreased by almost 65%. Also Eff shows a strong decrease with degradation time. Almost 65% of  $\eta$  has been lost after 3 hours, and only 9% of the initial  $\eta$  remained after 10 hours of degradation. The serial and shunt resistances,  $R_s$  and  $R_p$  respectively, are plotted in Figure 6.2C. The increase of  $R_s$  with degradation time happens simultaneously with the decrease of  $R_p$ . The obtained *jV*-curves are plotted in Figure 6.2D. From 0 to 6 hours of degradation, only a progressive decrease of  $J_{sc}$  is observed. At 6 hours and after 10 hours of degradation time, the decrease of  $J_{sc}$  is accompanied with a formation of an S-shaped *j*-*V* curve.

While Seeman et al. [33] showed in their study that degradation of the cell in presence of oxygen mainly results in the reduction of  $J_{sc}$ , Jorgensen et al. [42] mentioned the possible formation of an S-shaped *j*-*V* curve due to the degradation induced by water and its interaction

with the low work function electrodes and interfaces. The small drop (10%) of the  $V_{oc}$  which is representative of the electrode-semiconductor interface in the cell, together with the increase of  $R_s$  after 10 hours indicate a change at the electrode interfaces probably due to interactions with water molecules. The leakage current is determined by  $R_p$  and the turn on current is influenced by  $R_s$  as mentioned by Janssen et al. [53]. A larger  $R_p$  indicates a lower charge carrier recombination in the active layer and a smaller  $R_s$  indicates both a lower resistance of the semiconductor bulk resistance, and better metal/semiconductor interfaces as mentioned by Wang et al [54].

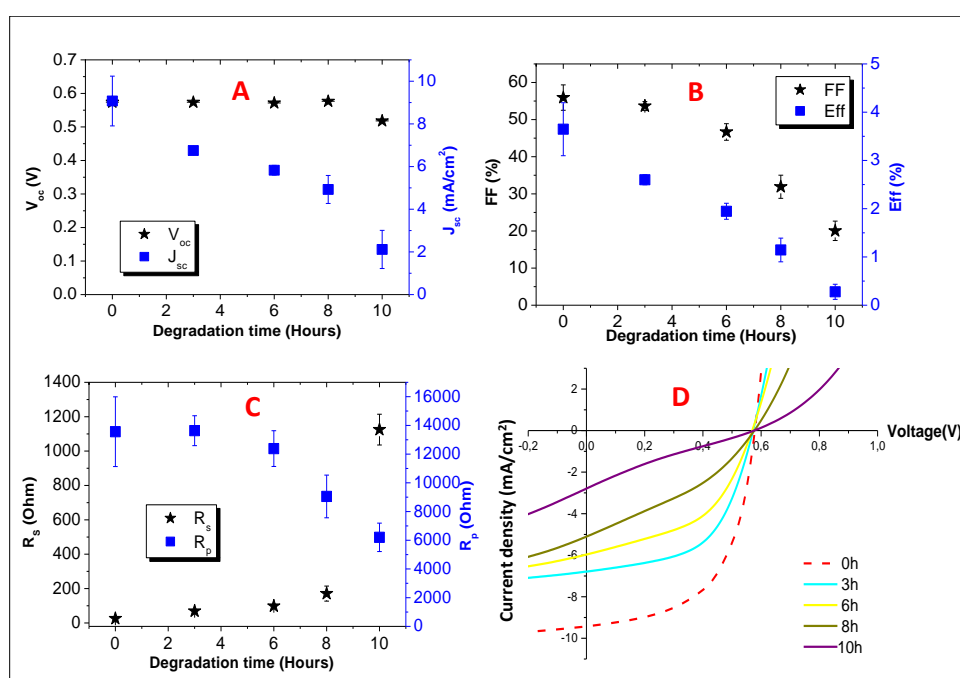


Figure 6.2. Evolution of the device parameters and  $j$ - $V$  curves with degradation time.

Also, it is known that the  $j$ - $V$  curve characteristics are severely distorted by the effect of  $R_s$ . In the case of significant value of  $R_s$ , this leads to a deformation of the  $j$ - $V$  curve shape and a distortion of the  $J_{sc}$  value [55].

To acquire more information about the degradation impact on the device performances, laser beam induced current (LBIC) technique has been applied. LBIC can be used to investigate degradation that occurs in organic solar cell devices by a mapping of the photocurrent density. This allows the detection of spatial inhomogeneities and defects which are present in the materials and which negatively affect the electrical performance of the solar cells. Figure 6.3 presents the LBIC images that have been recorded showing the spatial

distribution of the photocurrent density of a non-degraded solar cell (0 h) and of solar cell degraded for 2, 5 and 7 hours. The scanned area was approximately 6 mm x 3.5 mm and the solar cells were illuminated from the substrate side by the laser beam.

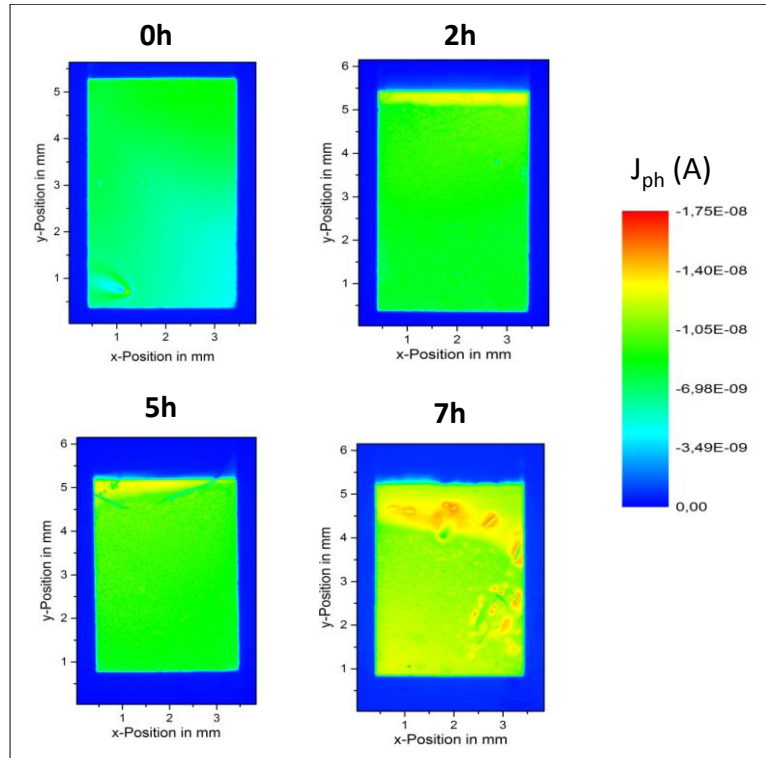


Figure 6.3. LBIC images showing the spatial distribution of the photocurrent density ( $J_{ph}$ ) of solar cells degraded for 0, 2, 5 and 7 hours.

The obtained results show an almost homogeneous distribution of the photocurrent for the non-degraded cell and for the device degraded for 2 hours. However, this homogeneity became disturbed after long degradation time. This is observed on the LBIC image for the cell degraded for 5 hours. It is even more visible on the LBIC image of the cell degraded for 7 hours. The measured photocurrent density did not considerably decrease with the degradation time as expected. Nevertheless, a number of features are observed on the most degraded solar cell (7 hours) where many isolated areas that looks like ‘‘islands’’ with high photocurrent density appeared. The formation of islands with higher efficiency is a characteristic feature of the well-known dark degradation of solar cells as reported by Jeranko et al. [37]. These features clearly show that degradation occurs by diffusion of water molecules through the rim of the solar cell device. The diffusion of water molecules are most probably the main reason of the observed inhomogeneities.

## VI.2.2. Degradation of single layer structures

In this experiment single layer structures, glass/ITO/PEDOT:PSS, are degraded first then the devices are finished by depositing the photoactive layer P3HT:PC<sub>60</sub>BM (1:0.7), the hole blocking layer (LiF) and the top electrode (Al). The results obtained during degradation are summarized in Figure 6.4.

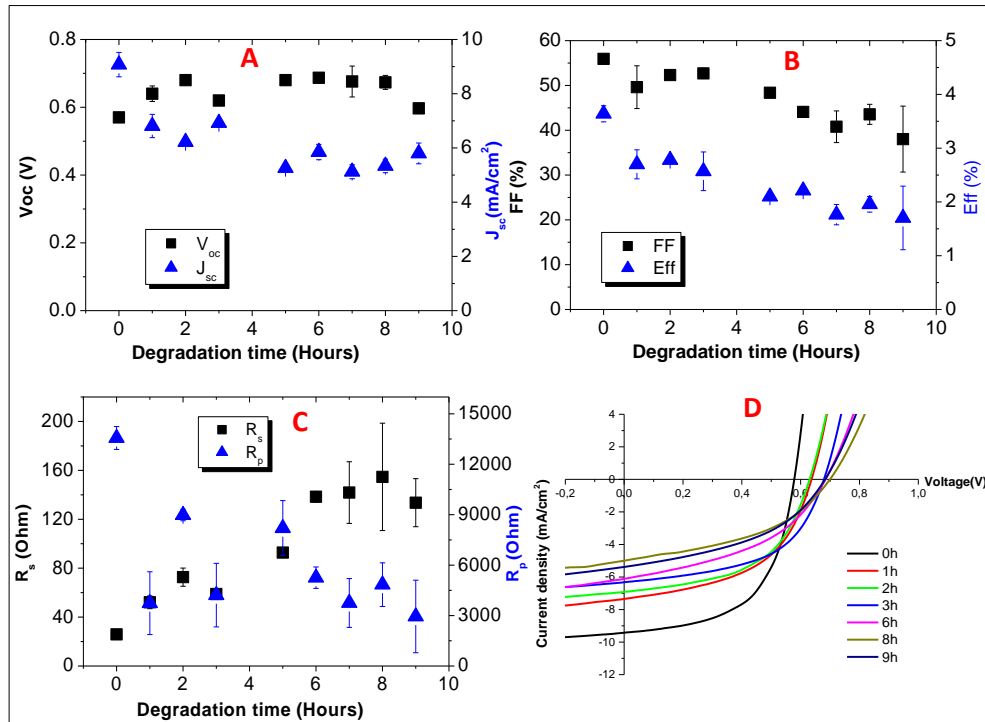


Figure 6.4. Evolution of the device parameters for different degradation times.

The  $V_{oc}$  (Figure 6.4A) is stable with degradation time. After the first 2 hours, the  $V_{oc}$  shows a slight increase before a decrease at 3 hours, after 5 hours the  $V_{oc}$  increased again and stayed almost constant until 9 hours of degradation. The  $J_{sc}$  (Figure 6.4A) showed a progressive decrease up to 5 hours and remained constant afterwards. After 9 hours, the  $J_{sc}$  has decreased by almost 35%. The FF and Eff (Figure 6.4B) decreased progressively with degradation time. Almost 28% of the initial FF value has been lost after 9 hours. The  $\eta$  showed a decrease of 27% after 1 hour, and almost 54% after 9 hours. The variation of the serial and shunt resistances,  $R_s$  and  $R_p$  respectively, with the degradation time is shown in Figure 6.4C. A random distribution of  $R_p$  is observed in the first 5 hours then  $R_p$  decreases

with the time of degradation. Simultaneously,  $R_s$  increase progressively. The decreasing of  $R_p$  and the increasing of  $R_s$  leads to a slight decrease of the  $V_{oc}$  and the  $J_{sc}$ , respectively. For both cases, this leads to a strong decrease of the electrical power that the cell delivers and therefore to a moderately decrease of the FF. In Figure 6.4D the  $jV$ -curves are plotted versus degradation time. The curves show a progressive decrease of  $J_{sc}$  in general. The formation of an S-shaped  $jV$ -curve, as it has been observed with multi-layer structure experiment, was not observed here. Also the degradation in the case of single-layer structures seems to be less pronounced than in the case of multi-layer structures.

## VII. Summary and Conclusions

In this thesis, a study of the degradation process of OSCs based on P3HT and a newly synthesized low-band p-type gap polymer named Si-PCPDTBT were studied under different degradation conditions such as photooxidation, damp-heat and photolysis. The study of the degradation process of inverted geometry OSCs of PEDOT:PSS/P3HT:PCBM/ZnO/ITO/Glass structure revealed interesting features. The acquired images of the PEDOT:PSS layer surface using different surface methods as SEM, AFM and OM show all similar features as presence of defects like holes, hills and needles and are more pronounced on the most aged sample. In one hand, it has been found that degradation process does not contribute to the density of holes indicating that holes in PEDOT:PSS are related to deposition process rather than to degradation itself. On the other hand, the defects on the PEDOT:PSS surface decorated by “white spots” or “white structures” of various size and shape that evolved with the degradation time could be correlated to chemical changes in the PEDOT:PSS. In addition, it was found that short term degradation (up to 2 hours) does not affect the PEDOT:PSS layer surface roughness and the SEM ion beam induce chemical degradation on P3HT:PCBM layer surface due to the highly used energy.

The SIMS depth profiles of structure degraded for 2h did not show any remarkable changes in the ion fragment yield, but integrated SIMS spectra showed some changes in different ion fragments attributed to the degradation process. It has been found that degradation leads to a strong intensity decreasing of ion fragments that are specific to the organic materials:  $C_xH_yS_z^-$  from the P3HT,  $C_xH_yO_z^-$  from the PEDOT:PSS and/or PCBM. In

parallel to the intensity decreasing of P3HT material, corresponding oxidized ion fragments ( $C_xH_ySO_z^-$ ) has been observed too highlighting on the degradation effect. The depth profiles obtained on the long term ageing (up to 210 hours) investigation revealed an increase of the oxygen ion fragment which is most probably due to the atmospheric oxygen incorporation during photooxidation. However, as previously discussed, the investigation of the PEDOT:PSS layer is very complex because the sulfur ( $S^-$ ) and carbon ( $C_3^-$ ) contains by both components (PEDOT and PSS).

The effect of damp-heat on the performance of solar cells consisting of P3HT:PCBM as photoactive layer materials has been investigated as well. The degradation of multi-layer structures results in a considerable drop of the power conversion efficiency from the initial value of 3.5 to 0.4 % after 10 hours of degradation. This corresponds to a loss of almost 90 %. In parallel, the fill factor decreased by almost 65%. Nevertheless, the open-circuit voltage is only moderately affected and decreased by about 10% within 10 hours of degradation. The short-circuit current showed a progressive decrease with degradation time. After 10 hours of degradation, only 24% of its initial value remained. The degradation is also accompanied with an increase of the serial resistance and with a decrease of the parallel resistance. The increase of the serial resistance indicates a deterioration of the interface electrode–semiconductor, while the decrease of the parallel resistance indicates an increase of the charge carrier recombination in the photoactive layer. The degradation results also in a formation of a S-shaped current-density curve caused by the interaction of water molecules with the low work function electrodes and the related interface. The obtained LBIC data show a degradation induced inhomogeneity distribution of the photocurrent density. These inhomogeneities are isolated areas with high photocurrents. This is a characteristic behavior of a well-known dark degradation. The degradation induced by water has been found to be partially reversible by thermal annealing at a temperature at 110°C under inert atmosphere (nitrogen). Similar results have been obtained with the degradation of single-layer structures. However, the observed degradation is less pronounced in the case of single-layer structures. Almost 50% of the initial power conversion efficiency remains after 9 hours of degradation, and the fill factor decreased by 30%. Also, no S-shaped current density-voltage curve formation has been observed even for long degradation times. This is probably due to the fact, as mentioned previously, that the formation of an S-shaped curve is caused by the interaction of water molecules with the low work function electrode and the related interface. This interaction is more likely in the case of a multi-layer structure.

The study of the degradation process of Si-PCPDTBT:PC<sub>70</sub>BM blend layers after different steps of photooxidation has been performed. It has been found that the atmospheric oxygen incorporation into the Si-PCPDTBT:PC<sub>70</sub>BM blend layers during photoassisted degradation lead to the inhomogeneous oxidation of the bulk, as it has been indicated from SIMS depth profiles of the layers at different degradation levels. The photooxidation effect resulting in UV absorbance loss lead to the degradation of the photoactive layer materials by a progressive increase of the oxidized ion species as NO<sup>-</sup>, SO<sup>-</sup>, NO<sub>2</sub><sup>-</sup>, SO<sub>2</sub><sup>-</sup> etc. In addition, the SIMS depth profiles reveal a remarkably enhanced photooxidation of the uppermost part of the photoactive layer. These features are in good agreement with the observation of new nano-objects (present as long chains of fibril form) on the photoactive layer surface as seen from the SEM images of the mostly degraded samples. Nevertheless, despite of the degradation, negligible surface roughness and good homogeneity of the layers between the nano-objects becomes preserved as revealed by AFM results.

The main objectives of the thesis that composes the investigation and explanation of the degradation mechanism of OSCs with the diverse characterization techniques used that provides complementary information, has been achieved. This led to a detailed investigation of relationship between chemical degradation at nano and macro-morphologies and eventually their correlation with the device performance loss. Also the degradation mechanism of organic-material under different condition (photooxidation, damp-heat and photolysis) based on the chemical evolution of the bulk heterojunction layer, the surfaces and interfacial layer were elucidate and thus related with the ageing and surface effects to nano-scaled interfacial variations.

To summarize, it has been found that the degradation of inverted geometry OSC structures at ambient atmosphere under photooxidation conditions affect mostly the PEDOT:PSS and P3HT:PCBM layer materials. Moreover, it has been shown that oxygen induces drastic changes of the device properties such as oxidation of materials, morphological changes and diffusion of interfacial layer toward semiconductors layer resulting in a deterioration of related interfaces and therefore results in a considerable loss of the device power conversion efficiency. Also, the obtained experimental results show, that water does induce substantial degradation in organic solar cells with a pronounced deterioration of the device properties. It has been found that the degradation occurs by diffusion of water molecules through the solar cell device which interacts with the low work function electrodes and related interface. This leads to the changes as the induced inhomogeneities observed with the photocurrent density of the aged samples resulting in a strong decrease of the power

conversion efficiency. We have found that for long-term ageing, the higher oxidation of the photoactive layer as it has been observed in the Si- PCPDTBT:PC<sub>70</sub>BM blend layer structures, could be an explanation of the total absence of photovoltaic response in the cells that has been described in the literature.

### **Main contribution of dissertation thesis:**

In correspondence with the objectives, the most important findings of the thesis can be summarized as follow:

- Complementary knowledge about the role of oxygen on the degradation process of the electron blocking layer PEDOT:PSS as well as the role of SEM ion beam on the degradation of P3HT:PCBM layer surface was gained.
- New scientific knowledge about the degradation process of the Si-PCPDTBT polymer under photooxidation conditions was achieved. The atmospheric oxygen incorporation into the Si-PCPDTBT:PC<sub>70</sub>BM blend layers during photoassisted degradation which lead to the inhomogeneous oxidation of the bulk, was proved from SIMS depth profiles.
- It has been found that for long-term ageing, the higher oxidation of the photoactive layer as it has been observed in the Si-PCPDTBT:PC<sub>70</sub>BM blend layer structures, could be an explanation of the total absence of photovoltaic response in the cells.
- Additional knowledge was gained on the roughness profile of PEDOT:PSS layer surface as well as Si-PCPDTBT:PC<sub>70</sub>BM blend layer structures under photooxidation conditions by using AFM method.
- Highlighting about the role of water on the degradation process of P3HT:PCBM solar cells: visualization of induced inhomogeneity distribution of the photocurrent density by LBIC.
- New knowledge about the effect of damp-heat on the device performance loss: the degradation is more pronounced in the case of multi-layers than single-layer structure. The interaction with water molecules is more likely in the case of multi-layers structure and therefore speeds up the degradation.

## References

- [1] Kasap and Capper, editors. Springer Handbook of Electronic and Photonic Materials. Springer.
- [2] Becquerel, A.E., Comptes Rendus, 9: 561–567 (1839).
- [3] Chapin, D.M., Fuller, C.S., Pearson, G.L., *J. Appl. Phys.*, 25: 676–677 (1954).
- [4] Hideki Shirakawa, Edwin J. Louis, Alan G. MacDiarmid, Chwan K. Chiang, and Alan J. Heeger, *J. Chem. Soc., Chem. Commun.*, 16, 578–580 (1977).
- [5] Belectric OPV GmbH (2012).
- [6] M.Seck, A. Distler, A. Vincze, D. Hasko, A. Satka and F. Uherek, In: Proc. of ADEPT, ISBN 978-80-554-0689-3 (2013).
- [7] K. Norrman, N.B. Larsen and F.C. Krebs, *Sol. Energ. Mat. Sol. Cells*, 90, 2793 (2006).
- [8] W. Prins, and J.J. Hermans, *J. Phys. Chem*, 63, 716–719 (1959).
- [9] K. Norrman, M.V. Madsen, S.A. Gevorgyan and F.C. Krebs, *J. Am. Chem. Soc*, 132, 16883–16892 (2010).
- [10] D. L. Staebler and C. R. Wronski, *Appl. Phys. Lett.*, 31(4), 292–294 (1977).
- [11] G. Yu, C. Zhang, and A. J. Heeger, *Appl. Phys. Lett.*, 64(12)1540–1542 (1994).
- [12] F. C. Krebs, ISBN 978-1-119-95251-0, *John Wiley & Sons*, Ltd (2012).
- [13] G. Chen, H. Sasabe, T. Sano, X-F. Wang, Z. Hong, J. Kido and Y. Yang, *Nanotechnology*, 24, 484007 (2013).
- [14] C. J. Brabec, S. E. Shaheen, T. Fromherz, F. Padinger, J. C. Hummelen, A. Dhanabalan, R. A. J. Janssen and N. S. Sariciftci, *Synth. Met*, 121, 1517–1520 (2001).
- [15] W. Brütting, *Physics of Organic Semiconductors*, Wiley-vch (2005).
- [16] J-G. Chen, H-Y. Wei and K-C. Ho, *Sol. Energ. Mat. Sol. Cells*, 91, 1472–1477 (2007).
- [17] A. Delcorte, *Appl. Surf. Sci*, 255, 954–958 (2008).
- [18] M.T. Dang, L. Hirsch and G. Wantz, *Adv. Mater*, 23, 3597–3602 (2001).
- [19] C.M. Bjorstrom, A. Bernasik, J. Rysz, A. Budkowski, S. Nilsson, M. Svensson, M. R. Andersson, K. O. Magnusson and E. Moons, *J. Phys.: Condens. Matter*, 17, L529–L534 (2005).
- [20] T.M. Clarke, J. Peet, P. Denk, G. Dennler, C. Lungenschmied, A.J. Mozer, *Energ. Environ. Sci.* 5, 5241–5245 (2012).
- [21] T.M. Clarke, D. B. Rodovsky, A.A. Herzing, J. Peet, G. Dennler, D. DeLongchamp, C. Lungenschmied, A. J. Mozer, *Adv. Energy Mater.* 1, 1062– 1067 (2011).
- [22] J. Peet, L. Wen, P. Byrne, S. Rodman, K. Forberich, Y. Shao, N. Drolet, R. Gaudiana, G. Dennler, D. Waller, *Appl. Phys. Lett.* 1, 98 (2011).
- [23] P. Würfel, *Chimia*, 61, 770–774 (2007).
- [24] H. Cao, W. He, Y. Mao, X. Lin, K. Ishikawa, J-H. Dickerson and W-P. Hess, *J. Power Sources*, 264, 168–183 (2014).
- [25] F. C. Krebs and H. Spanggaard, *Chem. Mater.*, 17(21):5235–5237 (2005).
- [26] H. Park, A. Roy, S. Beaupré, S. Cho, N. Coates, J. S. Moon, D. Moses, M. Leclerc, K. Lee, and A. J. Heeger, *Nat. Photonics*, 3, 297–303 (2009).
- [27] H. Y. Chen, J. Hou, S. Zhang, Y. Liang, G. Yang, Y. Yang, L. Yu, Y. Wu, and G. Li, *Nat. Photonics*, 3, 649–653 (2009).
- [28] M. Peach, In: optics.org, <http://optics.org/news/4/1/36> (2013).
- [29] M. V. Madsen, K. Norrman, and F. C. Krebs, *J. Photon Energy*, 1, 011104.1–011104.6 (2011).

- [30] C.J. Brabec, J.A. Hauch, P. Schilinsky and C. Waldauf, *MRS Bull*, 30, 50–53 (2005).
- [31] C.J. Brabec, *Sol. Energ. Mat. Sol. Cells*, 83, 273–292 (2004).
- [32] M.O. Reese, A.J. Morfa, M.S White, N. Kopidakis, S.E. Shaheen, G. Rumbles, D.S. Ginley, *Sol. Energ. Mat. Sol. Cells*, 92, 789 (2008).
- [33] A. Seeman, T. Sauermann, C. Lungenschmied, O. Armbrusters, S. Bauer, H-J. Egelhaaf and J. Hauch, *Solar Energy*, 85, 1238–1249 (2011).
- [34] S. Sarkar, J.H. Culp, J.T. Whyland, M. Garvan and V. Misra, *Org. Electron*, 11, 1896–1900 (2010).
- [35] B.M. Henry, A.G. Erlat, C.R.M Grovenor, G.A.D Briggs, T. Miyamoto and Y. Tsukahara, *In: Proceedings of the 46<sup>th</sup> Annual Technical Conference of the Society of Vacuum Coaters*, 600–605 (2003).
- [36] W. Prins, and J.J. Hermans, *J. Phys. Chem*, 63, 716–719 (1959).
- [37] T. Jeranko., H. Tributsch, N .S Sariciftcib and J. C. Hummelence, *Sol. Energ. Mat. Sol. Cells*, 83 (2–3), 247–262 (2004).
- [38] J. M. Kroon, M. M. Wienk, W. J.H. Verhees and J. C. Hummelen, *Thin Solid Films*, 403, 223–228 (2002).
- [39] T. Yamanari, T. Taima, J. Sakai, J. Tsukamoto and Y. Yoshida, *Jpn. J. Appl. Phys.*, 49 (1), 01AC02:4 (2010).
- [40] F.C. Krebs et al., *Sol. Energ. Mat. Sol. Cells*, 95 (5), 1348–1353 (2011).
- [41] K.A. Fynn et al., *IEEE Transactions on Electron Devices* 42 (10), 1775 (1995).
- [42] M. Jorgensen, K. Norrman and F. C. Krebs, et al., *Sol. Energ. Mat. Sol. Cells*, 92, 686–714 (2008).
- [43] F. C. Krebs, *Solar Cells*, Print ISBN: 9781119952510, *John Wiley & Sons*, Ltd (2012).
- [44] D. Mühlbacher, M. Scharber, M. Morana, Z. Zhu, D. Waller, R. Gaudiana and C. Brabec, *Adv. Mater.* 18, 2884–2889 (2006).
- [45] F. Deschler, D. Riedel, B. Ecker, E.V. Hauff, E.D. Como and R.C.I. Mackenzie, *Phys. Chem. Chem. Phys.* 15, 764–769 (2013).
- [46] G. Itskos, P. Papagiorgis , D. Tsokkou , A. Othonos , F. Hermerschmidt , S.P. Economopoulos, M. Yarema ,W. Heiss and S. Choulis, *Adv. Energy Mater.* 3, 1490–1499 (2013).
- [47] M. Scharber, M. Koppe, J. Gao, F. Cordella, and M. Loi, *Adv. Mat.*, 22(3): 367 (2010).
- [48] M. Morana, H. Azimi, G. Dennler, H-J. Egelhaaf, M. Scharber, Karen Forberich, Jens Hauch, R. Gaudiana, D. Waller, Z. Zhu, K. Hingerl, S. S. Bavel, J. Loos and C. Brabec, *Adv. Funct. Mater.*, 20(7): 1180–1188 (2010).
- [49] M-C. Scharber, M. Koppe, J. Gao, F. Cordella, M. A. Loi, P. Denk, M. Morana, H-J. Egelhaaf, K. Forberich, G. Dennler, R. Gaudiana, D. Waller, Z. Zhu, X. Shi, and C-J. Brabec, *Adv. Mater.* 22, 367–370 (2010).
- [50] M. Manceau, A. Rivaton, Jean-Luc Gardette, S. Guillerez, and N. Lemaitre. *Polym Degrad Stabil*, 94(6): 898–907 (2009).
- [51] A. Tournebize, P. O. Bussière, P. W. W. Chung, S. Thérias, A. Rivaton, J-L. Gardette, S. Beaupré and M. Leclerc, *Adv. Energy Mat.* 3, 478–487 (2013).
- [52] J.H Seo, S.Y. Nam, K.S Lee, T.D Kim and S. Cho, *Org. Electronics*. 13, 570-578 (2012).
- [53] RA. Janssen and J. Nelson, *Adv. Mater.* 25, 1847–1858 (2013).
- [54] Z. Wang, F. Zhang, L. Li, Q. An, J. Wang and J. Zhang, *Appl. Surf. Sci.* 305, 221– 226 (2014).
- [55] R. A. Street, K. W. Song, J. E. Northrup and S. Cowan, *Org. Electron.* 12, 244–248 (2011).

# List of publications

## CC. Publications

- Seck, M., A. Vincze, A. Satka, D. Hasko, F. Uherek, A. Tournebise, H. Peisert and T. Chasse, *Solar Energy Materials and Solar Cells* 132, 210-214 (2015).
- D. Begue, E. Guille, S. Mets, M-A. Arnaud, H-S. Silva, M. Seck, P. Fayon, C-D. Lartigau, P. Iratcabal, R-C. Hiorns, Graphene-based acceptor molecules for organic photovoltaic cells: a predictive theoretical and experimental study (*submitted to the Journal of the American Chemical Society, JACS*).
- A. Tournebise, M. Seck, T. Chasse, H. Peisert, A. Rivaton, A. Vincze, Photooxidation of Si-PCPDTBT:PC<sub>70</sub>BM active layer for organic solar cells applications: a surface and bulk investigation (*under submission process*).
- A. Isakova, M. Seck, S. Dowland, P. Topham, A. Sutherland, A. Vincze and D. Hasko, Cross-linked interlayers for stabilisation of organic solar cells (*under submission process*).

## Conferences and proceedings

- Seck, M., A. Distler, A. Vincze, D. Hasko, A. Satka, F. Uherek, Investigation of the degradation process in organic solar cell structures, 15<sup>th</sup> Conference of Doctoral Students (ELITECH 2013), ISBN 978-80-227-3947-4.
- Seck, M., A. Distler, A. Vincze, D. Hasko, A. Satka, F. Uherek, Study of degradation process in inverted organic solar cell structures, International Conference on Advances in Electronic and Photonic technologies (ADEPT 2013), book of proceedings, pp. 300-304, ISBN 9254-421-45214-45.
- Seck, M., combining surface and vertical profile-studies of materials in organic solar cell devices, FOTONIKA 2013, (2013) pp 55-58, ISBN 978-80-970493-5-5.
- M. SECK, A. TOURNEBISE, A. ŠATKA, A. VINCZE, D. HAŠKO, F. UHEREK, H. Peisert and T. Chasse, 8<sup>th</sup> international conference on Solid State Surfaces and Interfaces (SSSI 2013), book of proceedings, pp. 161-162, ISBN 978-80-223-3501-0.
- M. Seck, T. Stockinger, A. Satka, A. Vincze, D. Hasko, F. Uherek, R. Schwödianer, S. Bauer, Laser Beam Induced Current (LBIC) as a Characterization Tool of Organic Solar Cells Devices, FOTONIKA 2015, 51 (2015) pp. 37, ISBN 978-80-970493-8-6.
- M. Seck, S. Dowland, A. Vincze, D. Hasko, A. Šatka, F. Uherek, A. Distler, degradation study of organic solar based of KP115 using TOF-SIMS and SEM techniques, European conference on organic photovoltaic stability (ESOS), 8-11<sup>th</sup> June 2015.

